

Characteristics of UV-induced repair patches relative to the nuclear skeleton in human fibroblasts

Parimal Karmakar and Adayapalam T.Natarajan¹

MGC Department of Radiation Genetics and Chemical Mutagenesis, LUMC, Leiden University, Leiden, The Netherlands

We have tried to characterize the nucleotide excision repair (NER) events associated with the nuclear skeleton in both repair-proficient and repair-deficient human cell lines following UV irradiation. The repair patches were labelled with biotin-16-dUTP and the repair sites were visualized by fluorescence microscopy using fluorescence-conjugated antibodies to biotin. The intensities of repair labelling measured for the three human cell lines of normal, xeroderma pigmentosum group C (XP-C) and Cockayne syndrome group B (CS-B) are in good agreement with their known repair capabilities. Digestion of nuclei with DNase I markedly solubilized the repair patches in normal (3-fold reduction after 1 h post-UV incubation) and transcription-coupled repair (TCR)-defective Cockayne syndrome cells (6-fold reduction after 1 h post-UV incubation). The intensity of repair labelling remained the same in TCR-proficient XP-C cells after DNase I digestion, indicating that the repair events mediated by the TCR pathway are tightly associated with the nuclear skeleton. Treatment with ammonium sulphate after DNase I digestion further reduced the intensity of repair patches in both normal and Cockayne syndrome cells, but not in XP-C cells. The tight association of repair patches generated by the TCR pathway with the nucleoskeleton in XP-C cells reinforces the concept of functional compartmentalization of the nucleus, where NER is highly heterogeneous.

Introduction

The chromosomal DNA of higher eukaryotes is organized in the form of loops ranging in size from 60 to 80 kb with periodic attachment to a specific nuclear structure, known as the nuclear skeleton or matrix (Davie, 1995). The higher order chromatin organization of cellular DNA has important implications for different DNA metabolic activities such as replication, transcription, recombination and repair (Grasser and Laemmli, 1987). DNA repair is an important cellular function that maintains the genetic integrity by removing a wide variety of DNA damage induced by different environmental agents. In recent years efforts have been made to understand the mechanism of nucleotide excision repair (NER), which is one of the major repair pathways for the removal of bulky DNA adducts and DNA helix-distorting lesions. The dramatic consequences of defective NER are illustrated in certain human autosomal recessive disorders such as xeroderma pigmentosum (XP) and Cockayne syndrome (CS). XP involves seven different complementation groups (A–G) and many of these proteins are involved in the initial steps of the NER pathway (Sancar *et al.*, 1996).

The development of techniques to study repair in defined genomic regions has revealed that the NER process induced by UV radiation is highly heterogeneous across the genome. Actively transcribing regions are repaired faster than inactive regions (Bohr *et al.*, 1985; Selby and Sancar, 1993). This preferential repair has been attributed to proximal positioning of the genes with the transcription complex attached to the nuclear matrix (McCready and Cook, 1984). The preferential repair of active genes appears to be fairly independent of ongoing transcription (Svejstrup *et al.*, 1996), indicating that the close positioning of active genes to the nuclear matrix may be a prerequisite for rapid repair.

UV induces two major types of damage in the DNA, cyclobutane pyrimidine dimers (CPD) and 6–4 photoproducts (6–4 PP). These photolesions are not induced uniformly in the genome. 6–4 PP are introduced preferentially into non-nucleosomal DNA and this damage is rapidly removed from the genome overall without any bias towards the active genes, whereas UV-induced CPDs are preferentially removed from transcriptionally active genes by transcription-coupled repair (Venema *et al.*, 1992; Downes *et al.*, 1993).

NER is a co-ordinated sequence of events starting from DNA damage recognition to final ligation involving different proteins (Sancar, 1996). Cells defective in any of these proteins exhibit reduced repair activity. Studies on normal cells have revealed two pathways of NER: (i) transcription-coupled repair (TCR) and (ii) genome overall repair. UV-sensitive Cockayne syndrome cells are defective in global genome repair (Venema *et al.*, 1991; Hanawalt, 1994). Earlier studies on UV-induced repair labelling in nuclear halo preparations showed that the labelling was deficient in the nuclear matrix of CS cells while XP-C cells showed repair patches only in the nuclear matrix regions (Mullenders *et al.*, 1988). In these studies, nuclear halos were prepared by high salt extraction (2 M NaCl) of nuclei under non-physiological conditions.

There is increasing evidence showing that the regulatory elements of replication and transcription are attached to the nuclear skeleton. The newly synthesized RNA during transcription or DNA during replication are firmly attached to the skeleton (Jackson and Cook, 1986) which cannot be solubilized by DNase I digestion (Mullenders *et al.*, 1988; Jackson *et al.*, 1994a). It has already been shown that the enzymatic activities involved in NER are attached to chromatin (Bouayadi *et al.*, 1997). It is thus tempting to determine whether the repair events are attached to the skeleton. There has been, so far, only one report on the association of UV-induced preferential repair events with the nuclear matrix (Mullenders *et al.*, 1988).

In this study we have revisited the importance of the nuclear skeleton in the NER pathway in both CS-B and XP-C cells by adopting a quasi *in vitro* assay which closely mimics the *in vivo* conditions. In this technique, agarose embedded cells were permeabilized to carry out cellular activity like replication

¹To whom correspondence should be addressed at: Department of Radiation Genetics and Chemical Mutagenesis, Sylvius Laboratory, State University of Leiden, PO Box 9503, 2300 RA Leiden, The Netherlands. Tel: +31 7152 76164; Fax: +31 7152 21615; Email: natarajan@rullf2.medfac.leidenuniv.nl

and transcription with biotin- or bromine-labelled precursors. The incorporated sites were localized by indirect immunolabelling. This method has been used successfully to visualize UV-induced repair patches (Jackson *et al.*, 1994b). We have tried to address the role of the nucleoskeleton in NER using a gentle approach to keep the cellular structure intact and visualizing the repair patches directly under a microscope (Jackson *et al.*, 1988), choosing XP-C and CS-B cells to critically evaluate the importance of the nuclear skeleton in the TCR pathway.

Material and methods

Cell cultures

Normal human (VH25), XP-C (XP21RO) and CS-B (CSIAN) fibroblasts were used in the present study. All the cells were maintained in medium F10 supplemented with 10% fetal bovine serum and antibiotics at 37°C in an incubator under a 2.5% CO₂ atmosphere. Cells were grown in culture flasks until they became confluent. Cells were kept confluent for 3 days without changing the medium prior to the experiment.

UV irradiation

The cells were irradiated at room temperature using a Philips TUV lamp at a dose rate of 0.2 J/m²/s.

Encapsulation and permeabilization of the cells

Trypsinized cells were encapsulated in agarose as described by Jackson *et al.* (1994). Briefly, confluent cells were trypsinized and resuspended in phosphate-buffered saline (PBS) at a concentration of 2×10⁵ cells/ml. Cell suspension in PBS was mixed gently with an equal volume of 1% low gelling agarose (Sigma) at 39°C. An equal volume of paraffin oil was mixed thoroughly with this and kept on ice for 1 min. The whole mixture was kept at room temperature for 5 min. Finally, they were centrifuged repeatedly to remove the paraffin oil. Formation of beads was checked under a phase contrast microscope. Each bead contained between five and eight cells. The beads were incubated further in PBS at 37°C for 1 h before irradiation. Irradiated or unirradiated beads containing cells were kept in conditioned medium for different times at 37°C. After incubation they were washed twice with PBS and three times with cold physiological buffer (PB) [100 mM KH₂PO₄, 130 mM KCl, 10 mM Na₂PO₄, 1 mM MgCl₂, 1 mM Na₂ATP (type II; Sigma), 1 mM DTT, pH 7.4]. The beads were then incubated with 5 IU/ml streptolysin O (SLO) (Wellcome) on ice for 15 min, then washed with cold PB to remove unbound SLO. The beads were then incubated for 1 min at 37°C and then washed twice with cold PB. The cells in the beads were now permeabilized and ready for the repair reaction.

Labelling of repair patches

Irradiated or unirradiated agarose embedded permeabilized cells were then incubated with 10× repair mix containing 2.5 mM each dGTP, dCTP and dATP and 100 μM biotin-16-dUTP (Boehringer Mannheim), 50 mM phosphate buffer, pH 7.4, and 2.5 mM MgCl₂ for 15 min at 37°C. After 1 h the reaction was stopped with cold PB and washed three times with cold PB. The beads were then incubated on ice with an equal volume of 0.5% Triton in PB for 10 min and washed three times with PB.

Preparation of the nuclear skeleton

The cells in the beads which had incorporated biotin were then digested with 200 IU/ml DNase (Sigma) at 37°C for 1 h. Such digestion removes 90% of the cellular DNA as observed by agarose gel electrophoresis (data not shown). After digestion the beads were washed with cold PB three times and finally incubated with 0.25 M ammonium sulphate to extract cellular proteins other than the skeleton (Davie, 1995). Finally the beads were washed extensively with cold PB.

Fixation and immunolabelling

After several washes the cells were fixed with 2% formaldehyde for 15 min at room temperature. Finally the beads were incubated with 1% BSA and 1% goat serum for 30 min at room temperature and washed with wash buffer (PB containing 0.5% Tween-20 and 0.1% BSA) once. The sites containing the biotin were detected using avidin-FITC (1:500 dilution; Sigma) by incubation at room temperature for 30 min followed by further incubation at room temperature for 30 min with goat anti-avidin (1:200 dilution; Sigma), and finally the beads were incubated with avidin-FITC again for 30 min at room temperature. After each incubation the beads were washed three times with wash buffer. Aliquots of 25 μl of beads were mounted under a coverslip in Vectashield (Vector Laboratories). The slides were immediately viewed under an Axioplan fluorescence microscope (Zeiss). Images were captured using a Nu 200 CCD camera (Photometric) linked to an Apple Power Computer. For

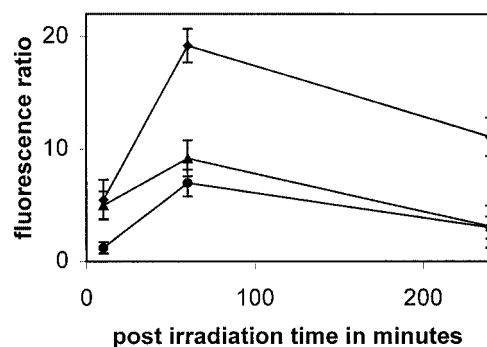


Fig. 1. Effect of different post-UV incubation times on repair patches for different cells. For each point at least 30–50 nuclei were taken and the fluorescence ratio was calculated after normalizing the values to the unirradiated control. Agarose embedded cells were irradiated with 10 J/m²/s UV and incubated for different times and the cells were then permeabilized and repair reactions were carried out in the presence of DNA precursors containing biotin-16-dUTP. The sites of incorporated biotin were visualized after indirect immunolabelling sequentially with avidin-FITC, anti-avidin and finally avidin-FITC. The slides were processed immediately and total fluorescence ratios were calculated using IBLab spectrum. Normal, ○; CS-B, ◆; XP-C, ▲.

the determination of fluorescence intensity nuclei were selected randomly and total intensity was measured using IPLab Spectrum software.

Proliferating cell nuclear antigen (PCNA) immunolabelling

Agarose embedded confluent cells were irradiated with UV and incubated for different times. After incubation the cells were washed twice with PBS and twice with cold PB. The beads were then incubated with cold PB containing 0.5% Triton for 10 min at 4°C. The coverslips were then washed four times with PB and fixed with methanol for 15 min at –20°C. The fixed cells were then washed and incubated with mouse monoclonal anti-PCNA antibody (1:100 dilution; Sigma) for 30 min at room temperature. The cells were washed with PB containing 0.5% Tween-20 three times, followed by a further 30 min incubation at room temperature with donkey anti-mouse IgG conjugated with FITC (1:100; Jackson Laboratories) in the dark. The beads were then washed three times in wash buffer and mounted in Vectashield (Vector Laboratories). The slides were viewed under a fluorescence microscope. The images were analysed using the method described above.

Results

We have documented here the characteristics of UV-induced repair patches in different human fibroblast cell lines using an *in vitro* assay under near physiological conditions. The cells were encapsulated in agarose microbeads to protect the chromatin from shearing and upon permeabilization such cells can perform repair and transcription efficiently. This method has earlier been used to successfully visualize UV-induced repair patches and transcription foci (Jackson *et al.*, 1994a).

We have measured the fluorescence intensity of repair patches from different cells (Figure 1). The cells were irradiated with 10 J/m²/s and incubated in the same medium for different post-irradiation times. At least 30–50 nuclei were chosen randomly for each time point and the fluorescence ratio was measured by normalizing the data from each point to an unirradiated control. As confluent fibroblast cells were used, there was no repair labelling in the unirradiated control. The number of cells in S phase was not more than 1%, and the signal from such S phase cells was much more intense than repair labelling and could be easily differentiated from that of repair. S phase cells were excluded from the analysis. In all the three cell lines used the fluorescence intensity of repair increased up to 1 h and then decreased slowly. Repair sites were readily visualized even after 15 min in the case of normal and CS-B cells, while XP-C cells required a minimum of 1 h post-UV incubation to visualize the repair patches.

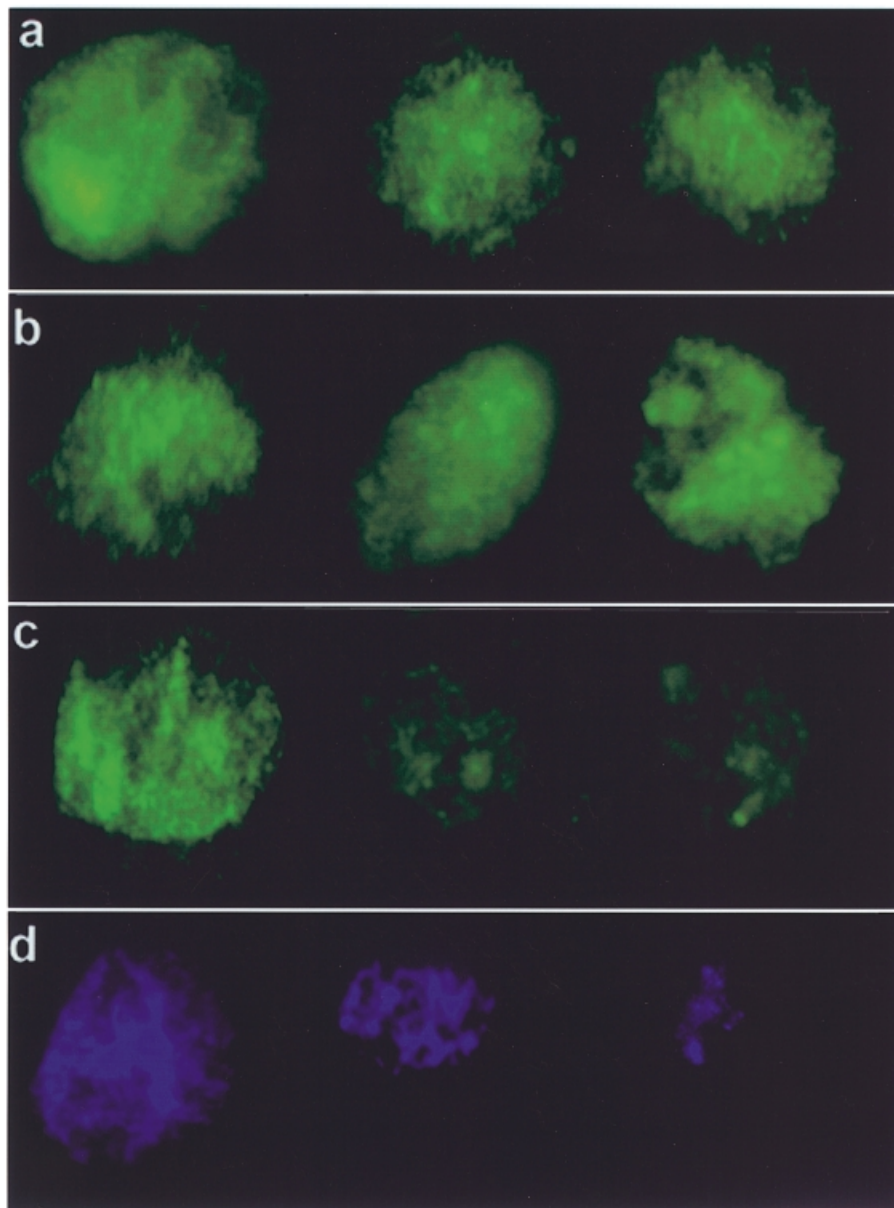


Fig. 2. Fluorescence microscopic pictures of UV-induced repair patches for different cells. Agarose embedded cells were irradiated with $10 \text{ J/m}^2/\text{s}$ UV and incubated for 1 h. The cells were then permeabilized and repair reactions were carried out in the presence of DNA precursors containing biotin-16-dUTP. The sites of incorporated biotin were visualized as repair patches by indirect immunolabelling (a). (b) UV-irradiated cells digested with DNase after completion of the repair reaction. (c) UV-irradiated cells digested with DNase followed by ammonium sulphate extraction. (d) Cells with DAPI staining. In each case the residual sites of repair patches were visualized after indirect immunolabelling. The first row represents normal cells, the second row XP-C cells and the third row CS-B cells.

The representative pictures of different cells after 1 h post-UV incubation are presented in Figure 2. Rows 1–3 represent normal, XP-C and CS-B cells, respectively. Columns (a)–(c) represent, respectively, repair patches alone, the same with DNase digestion and with DNase + ammonium sulphate extraction. As there was no signal from unirradiated cells, DAPI stained nuclei are shown as a control for normal cells in column 4. As each repair patch consists of nearly 30 nucleotides, on average eight biotin molecules are expected to be incorporated. The repair foci were small and scattered over the whole nucleus except for the nucleolus. In the case of XP-C and CS-B cells the intensity of the signal was lower than normal. After DNase digestion, there was a 3-fold reduction in the fluorescence intensity of repair labelling in normal cells.

CSB cells, on the other hand, showed a 6-fold decline in the intensity of repair labelling. In the case of XP-C cells, which are proficient in the TCR pathway, there was no decrease in the intensity after DNase digestion. After ammonium sulphate extraction the signal completely vanished from CS-B cells. While in normal cells the intensity was reduced further, in XP-C cells there was no reduction in the signal.

We have plotted the fluorescence ratio for the three cell types at different post-UV incubation times (Figure 3). At each time point, the cells were digested with DNase and ammonium sulphate to visualize the association of repair and the nuclear skeleton. At 10 min post-UV irradiation, repair sites were not detectable in XP-C cells owing to the limited capacity to repair both CPDs and 6–4 PP in the transcribing

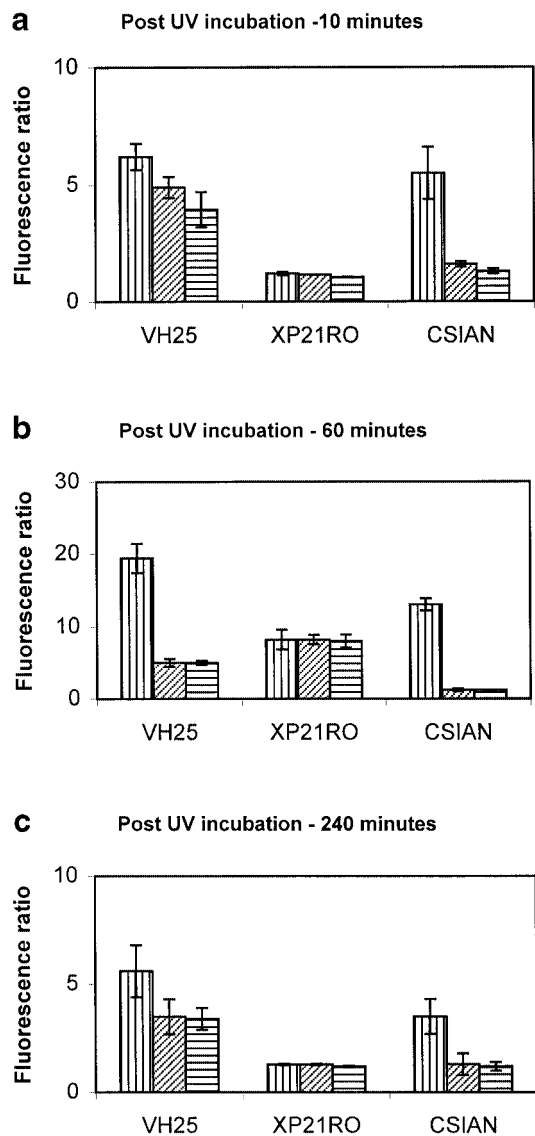


Fig. 3. Effect of DNase digestion and ammonium sulphate extraction on different cells. Agarose embedded cells were irradiated with $10 \text{ Jm}^2/\text{s}$ UV and incubated for different times before the repair reaction was carried out. The reaction was stopped by adding cold PB, the cells were then digested with DNase, followed by ammonium sulphate extraction. (a) The fluorescence ratio after DNase digestion or DNase + ammonium sulphate treatment in three cell lines after 10 min post-UV incubation. (b) As (a) with a post-UV incubation time of 1 h. (c) Post-UV incubation for 4 h. UV, ▨; UV + DNase, ▩; UV + DNase + ammonium sulphate, ▪.

strand of active genes. Repair patches were reduced significantly after digestion with DNase or ammonium sulphate in CS-B cells but in normal cells there was little effect of DNase or ammonium sulphate treatment.

In Figure 3b and c the fluorescence ratios of repair patches are shown for the three cell types after DNase digestion followed by ammonium sulphate extraction for 1 and 4 h post-UV incubation. In XP-C cells, the relative fluorescence intensity of repair labelling was unaffected by either DNase I digestion or DNase I + ammonium sulphate extraction. This indicates that the patches generated by the TCR pathway are tightly associated with the nucleoskeleton. In normal cells the fluorescence ratio was reduced 3-fold after DNase digestion followed by ammonium sulphate extraction 1 h post-UV irradiation. For CS-B cells the fluorescence ratio was reduced

6-fold after DNase digestion followed by ammonium sulphate extraction. After 4 h post-UV incubation XP-C cells did not show any decrease in fluorescence ratio after digestion with DNase followed by ammonium sulphate extraction. In this case, for CS-B cells the fluorescence ratio decreased 2.5 times but in normal cells the fluorescence ratio was reduced 1.5 times.

In order to determine the role of PCNA in these repair events we labelled PCNA in UV-irradiated cells (Figure 4). Such PCNA immunolabelling was found to be an alternative approach to assess NER capability (Aboussekhra and Wood, 1995). After digestion with DNase the PCNA immunostaining remained the same in XP-C cells but CS-B cells showed considerably reduced signal. This observation was consistent with the repair patches. However, after treatment with ammonium sulphate, all the PCNA was washed out, leaving the nuclear skeleton (Davie, 1995), and there was no signal from cells after such treatment (data not shown).

In some control experiments we used NER-defective XP-A cells. Both repair patches and PCNA immunostaining were absent in XP-A cells after UV irradiation, indicating that our observations were not due to an experimental artefact.

Discussion

In this study, attempts have been made to find an association of UV-induced repair with the nucleoskeleton in human fibroblast cell lines with different repair characteristics. Earlier studies to visualize repair events with respect to the nuclear skeleton (Jackson *et al.*, 1994a,b) were confined to normal cells. We have used a gentle method for the analysis of repair in intact chromatin. This method has been adopted successfully to visualize the transcription and repair foci induced by UV (Jackson *et al.*, 1993, 1994a,b). Agarose embedded permeabilized cells can efficiently perform transcription, replication and repair. All these processes are presumably attached to the nuclear skeleton. It has already been shown that the resynthesis step of NER is tightly bound to chromatin (Bouayadi *et al.*, 1997). As a further step, we have here tried to document a distinct association of NER subpathways with the nuclear skeleton.

It is very well established that UV-induced repair is highly heterogeneous in the genome. McCready and Cook (1984) showed that the initial repair events take place at the nuclear cage or matrix. This observation is very much analogous to replication and transcription, where nascent RNA and DNA synthesis primarily occurs at the matrix. Although the initial repair occurs at the matrix, the majority of the repair sites labelled *in vitro* are moved in normal cells. This suggests that only a fraction of repair patches are tightly associated with the skeleton. It is not clear which of the two subpathways of NER, i.e. TCR or global genome repair, is associated with the nucleoskeleton.

The preferential repair of transcriptionally active regions has been attributed to the fact that these regions are proximal to the transcription machinery (Mullenders *et al.*, 1988). The repair reactions of UV-induced damage have distinct characteristics. *In vitro* repair labelling revealed that repair patches are randomly distributed in the nucleus (Jackson *et al.*, 1994a). Evidence is now accumulating that the transcription apparatus and replication factories are attached to the skeleton and thus the newly synthesized DNA or RNA is not sensitive to DNase digestion (Hozak *et al.*, 1993; Jackson *et al.*, 1993). It seems likely from our observations that the repair reaction

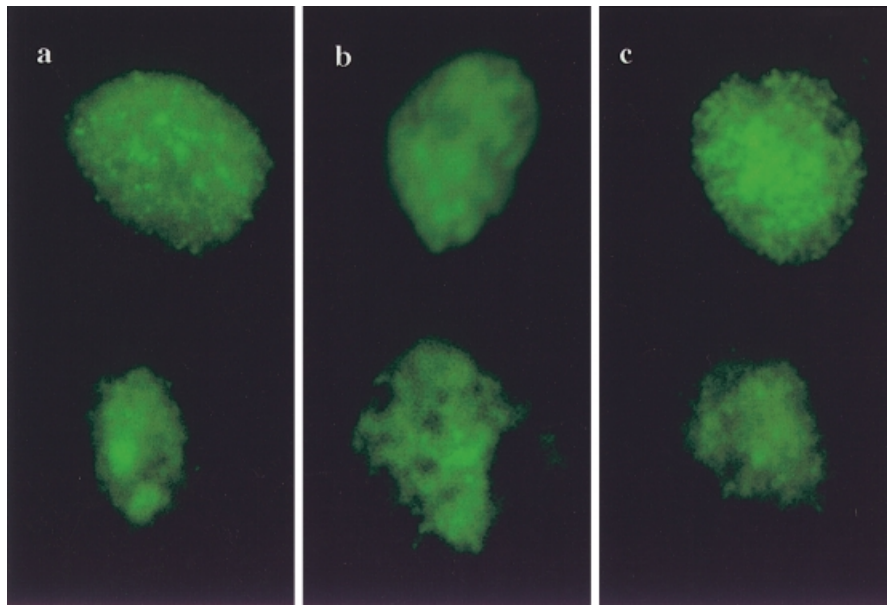


Fig. 4. Immunolabelling of PCNA in UV-irradiated cells. Agarose embedded cells were irradiated with $10 \text{ J/m}^2/\text{s}$ and incubated for 1 h. After incubation cells were lysed with Triton in PB and PCNA was immunolabelled with mouse anti-PCNA antibody (Sigma) (a). Cells after lysing with Triton were digested with DNase and then PCNA was immunolabelled (b). When such cells were further treated with ammonium sulphate there were no signals for PCNA (c).

mediated by the TCR pathway is firmly attached to the skeleton. This may perhaps explain the rapid repair of active genes, as these regions are proximal to the transcription apparatus. The transcription factor TFIIF plays an active part not only in TCR but also in global genome repair (Lehmann, 1995). We have seen that the repair rate is slow in XP-C cells at first, whereas it is rapid in normal cells. This is probably due to the rapid removal of 6–4 PP only from the transcriptionally active strand in XP-C cells.

The enzymatic steps involved in NER are tightly associated with chromatin and such an association is mediated by PCNA (Bouayadi *et al.*, 1997). We have also tried to find a possible association of PCNA with repair in different cells. It has already been shown that UV-induced repair patches co-localize with PCNA. PCNA was found to be associated with damaged DNA in a detergent-resistant form after UV irradiation (Pagano *et al.*, 1994). Involvement of PCNA with the repair events is also observed in our case and the involvement is dependent on the NER subpathway. However, if the repair patches subject to TCR are attached to the skeleton then part of the PCNA involved in this repair pathway is expected to be resistant to DNase I digestion. We found that in TCR-proficient XP-C cells, a fraction of PCNA was resistant to digestion with DNase I. Similarities observed between the DNase-resistant repair patches and PCNA in XP-C tend to suggest that the TCR pathway occurs in close association with the nucleoskeleton. This possibility is strengthened by the fact that CS-B cells, deficient in TCR, did not show any retention of repair patches and PCNA after DNase I digestion. As normal human cells are proficient in both the global genome and TCR pathways, they exhibit an intermediate state between XP-C and CS-B cells.

Acknowledgements

We thank Prof. U. Dasgupta (Department of Biophysics, Calcutta University) for critical reading of the manuscript. We are grateful to Jan Boie for his help in the computer analysis. This research was funded by an EU Nuclear Safety project to A.T.N.

References

- Aboussekhra, A. and Wood, R.D. (1995) Detection of nucleotide excision repair incisions in human fibroblasts by immunostaining for PCNA. *Exp. Cell Res.*, **221**, 326–332.
- Bohr, V.A., Smith, C.A., Okumoto, D.S. and Hanawalt, P.C. (1985) DNA repair in an active gene: removal of pyrimidine dimers from the DHFR gene of CHO cells is much more efficient than in the genome overall. *Cell*, **40**, 359–369.
- Bouayadi, K., VanHoffen, A., Balajee, A.S., Natarajan, A.T., VanZeeland, A.A. and Mullenders, L.H.F. (1997) Enzymatic activities involved in the DNA resynthesis step of nucleotide excision repair are firmly attached to chromatin. *Nucleic Acids Res.*, **75**, 1056–1063.
- Davie, J.M. (1995) The nuclear matrix and the regulation of chromatin organisation and function. *Int. Rev. Cytol.*, **162A**, 191–251.
- Downes, C.S., Ryans, A.J. and Johnson, R.T. (1993) Fine tuning of DNA repair in transcribed genes: mechanisms, prevalence and consequences. *Bioessays*, **15**, 209–216.
- Grasser, S.M. and Laemmli, U.K. (1987) A glimpse at chromosomal order. *Trends Genet.*, **2**, 16–22.
- Hanawalt, P.C. (1994) Transcription-coupled repair and human disease. *Science*, **266**, 1957–1959.
- Hozak, P., Hassan, A.B., Jackson, D.A. and Cook, P.R. (1993) Visualisation of replication factories attached to nucleoskeleton. *Cell*, **73**, 361–373.
- Jackson, D.A. and Cook, P.R. (1986) Replication occurs at a nucleoskeleton. *EMBO J.*, **5**, 1404–1410.
- Jackson, D.A., Hassen, A.B., Errington, R.J. and Cook, P.R. (1993) Visualisation of focal sites of transcription within human nuclei. *EMBO J.*, **12**, 1059–1065.
- Jackson, D.A., Balajee, A.S., Mullenders, L.H.F. and Cook, P.R. (1994a) Sites in human nuclei where DNA damaged by ultraviolet light is repaired: visualisation and localisation relative to the nucleoskeleton. *J. Cell Sci.*, **107**, 1745–1752.
- Jackson, D.A., Hassen, A.B., Errington, R.J. and Cook, P.R. (1994b) Sites in human nuclei where damage induced by ultraviolet light is repaired: localisation relative to transcription sites and concentrations of proliferating cell nuclear antigen and the tumour suppressor protein, p53. *J. Cell Sci.*, **107**, 1753–1760.
- Jackson, D.A., Yuan, J. and Cook, P.R. (1988) A gentle method for preparing cyto- and nucleoskeletons and associated chromatin. *J. Cell Sci.*, **90**, 365–378.
- Lehmann, R.A. (1995) Nucleotide excision repair and the link with transcription. *Trends Biochem. Sci.*, **20**, 402–405.
- McCready, S.J. and Cook, P.R. (1984) Lesions induced in DNA by ultraviolet light are repaired at the nuclear cage. *J. Cell Sci.*, **70**, 189–196.
- Mullenders, L.H.F., van Kersteren, A.C., van Zeeland, A.A. and Natarajan, A.T. (1988) Nuclear matrix associated DNA is preferentially repaired in normal

- human fibroblasts, exposed to a low dose of ultraviolet light but not in Cockayne's syndrome fibroblasts. *Nucleic Acids Res.*, **16**, 10607–10622.
- Pagano,M., Theodoras,A.M., Tam,S.W. and Draetta,G.F. (1994) Cyclin D1-mediated inhibition of repair and replicative DNA synthesis in human fibroblasts. *Genes Dev.*, **8**, 1627–1639.
- Sancar,A. (1996) DNA excision repairs. *Annu. Rev. Biochem.*, **65**, 43–81.
- Sancar,G.B., Siede,W. and van Zeeland,A.A. (1996) Repair and processing of DNA damage: a summary of recent progress. *Mutat. Res.*, **362**, 127–146.
- Selby,C.P. and Sancar,A. (1993) Molecular mechanism of transcription-repair coupling. *Science*, **260**, 53–58.
- Svejstrup,J.S., Vinchi,P. and Eagly,J.M. (1996) The multiple roles of transcription/repair factor TFIIH. *Trends Biochem. Sci.*, **21**, 346–350.
- Venema,J., Vanhoffen,A., Karcagi,V., Natarajan,A.T., VanZeeland,A.A. and Mullenders,L.H.F. (1991) Xeroderma pigmentosum complementation group C cells remove pyrimidine dimers selectively from the transcribed strand of active genes. *Mol. Cell. Biol.*, **11**, 4128–4134.
- Venema,J., Bastosova,Z., Natarajan,A.T., VanZeeland,A.A. and Mullenders,L.H.F. (1992) Transcription affects the rate but not the extent of repair of cyclobutane pyrimidine dimers in the human adenosine deaminase gene. *J. Biol. Chem.*, **267**, 8852–8856.

Received on July 29, 1999; accepted on November 4, 1999